View metadata, citation and similar papers at core.ac.uk

brought to you by CORE

provided by Elsevier - Publisher Connector

Available online at www.sciencedirect.com

ScienceDirect

Publishing Services by Elsevier

International Journal of Naval Architecture and Ocean Engineering 8 (2016) 243–251

http://www.journals.elsevier.com/international-journal-of-naval-architecture-and-ocean-engineering/

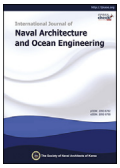

Thruster fault diagnosis method based on Gaussian particle filter for autonomous underwater vehicles

Yu-shan Sun*, Xiang-rui Ran, Yue-ming Li, Guo-cheng Zhang, Ying-hao Zhang

Science and Technology on Underwater Vehicle Laboratory, Harbin Engineering University, Harbin, 150001, China

Received 14 August 2015; revised 21 September 2015; accepted 28 January 2016
Available online 9 May 2016

Abstract

Autonomous Underwater Vehicles (AUVs) generally work in complex marine environments. Any fault in AUVs may cause significant losses. Thus, system reliability and automatic fault diagnosis are important. To address the actuator failure of AUVs, a fault diagnosis method based on the Gaussian particle filter is proposed in this study. Six free-space motion equation mathematical models are established in accordance with the actuator configuration of AUVs. The value of the control (moment) loss parameter is adopted on the basis of these models to represent underwater vehicle malfunction, and an actuator failure model is established. An improved Gaussian particle filtering algorithm is proposed and is used to estimate the AUV failure model and motion state. Bayes algorithm is employed to perform robot fault detection. The sliding window method is adopted for fault magnitude estimation. The feasibility and validity of the proposed method are verified through simulation experiments and experimental data.

Copyright © 2016 Society of Naval Architects of Korea. Production and hosting by Elsevier B.V. This is an open access article under the CC BY-NC-ND license (http://creativecommons.org/licenses/by-nc-nd/4.0/).

Keywords: Autonomous Underwater Vehicle (AUV); Thruster; Fault diagnosis; Gaussian particle filter

1. Introduction

Autonomous Underwater Vehicles (AUVs) have been increasingly applied globally for scientific exploration, marine development, and underwater engineering, among other applications (Mai et al., 2014; Gafurov and Klochkov, 2015). Given future expansion prospects in marine development and maritime research, AUVs are vital in obtaining underwater information and for precision strikes and asymmetric intelligence warfare. Underwater vehicle technology has also become a hot research topic worldwide (Mai et al., 2014; Gafurov and Klochkov, 2015).

AUVs usually implement various tasks in complex marine environments, but the occurrence of faults may cause significant losses. Therefore, an intelligent robot that can deal with emergencies is required, that is, it should be able to perform automatic fault diagnosis and have fault-tolerant control abilities. The autonomous fault diagnosis and fault-tolerant control ability of AUVs are important to guarantee the autonomy, reliability, and adaptability of AUVs in the ocean. AUV fault diagnosis objects include sensors, actuators, and control systems. The normal function of an AUV is the foundation for its ability to complete tasks. The thruster of an AUV is the driving force actuator; the AUV is unpredictable and dangerous if a fault occurs and is not diagnosed or treated promptly. During a serious case, an AUV cannot complete missions and tasks properly, thereby leading to disastrous consequences.

Frank, a German professor who is an international fault diagnosis authority, categorized fault diagnosis methods into three: analytical model based, signal processing based, and knowledge based (Frank, 1990). The analytical model-based method is the earliest and most systematic fault diagnosis method; this method can further analyze the natural dynamic characteristics of a system and is conducive to real-time diagnostics, fault location and separation, and early fault diagnosis. Matko et al. (2012) presented an implementation of

* Corresponding author.
E-mail address: sunys2000@126.com (Y.-s. Sun).
Peer review under responsibility of Society of Naval Architects of Korea.

http://dx.doi.org/10.1016/j.ijnaoe.2016.03.003
2092-6782/Copyright © 2016 Society of Naval Architects of Korea. Production and hosting by Elsevier B.V. This is an open access article under the CC BY-NC-ND license (http://creativecommons.org/licenses/by-nc-nd/4.0/).

Sigma-Point Unscented Kalman Filter (SP-UKF) used in a simulated open-water navigation task of two types of AUV. Yuan et al. (2011) used reduced-order Kalman filter to estimate the fault size of an actuator online; this filter can be applied in fault tolerant control. AUV is a strong nonlinear system; the use of the Gaussian particle filter is this system can solve this kind of problem (Hutt and Dearden, 2003; Sadeghzadeh Nokhodberiz and Poshtan, 2014) and avoid shortcomings, such as general filter particle degradation and sample impoverishment (Schmal and Cheng, 2015). Compared with the Extended Kalman Filter (EKF) and UKF, the Gaussian particle filter has better treatment effects in solving nonlinear problems (Freitas et al., 2004), and this filter can handle non-Gaussian noise problems (Yafe et al., 2014). Hutter and Dearden (2003) attempted to employ the Gaussian particle filter to diagnose faults online.

This study uses an improved Gaussian particle filter to estimate AUV fault model parameters and motion state. It uses modified Bayesian algorithms to detect faults. The thruster fault diagnosis method, which uses a sliding window to estimate the magnitude, is also employed. Simulation and sea trial experimental data are used to verify the accuracy and feasibility of this method.

2. AUV platform and mathematical modeling

2.1. Brief introduction to the AUV platform

ZS-AUV is equipped with various acoustic detection sensors. And it can perform different underwater exploration tasks. The dimensions and specifications of the AUV are shown in Table 1.

The implementing agent of ZS-AUV adopts the thruster method and is equipped with eight thrusters. In accordance with the force functions, the thrusters can be grouped into four: horizontal main thruster, vertical plain main thruster, vertical thruster, and lateral thruster; each group comprises two thrusters. The AUV thruster configuration is shown in Figs. 1 and 2. The main horizontal thruster adopts a catheter thruster, in which the maximum thrust of the main thruster is 100 kgf, the maximum reverse thrust is 37 kgf, and the maximum input power is 5 kW; the longitudinal axis of the thruster and that of the vehicle form a 13° angle. The maximum thrust of the vertical main thruster is 25 kgf, the maximum reverse thrust is 14.5 kgf, the maximum input power is 1 kW, and the longitudinal axis of the thruster and that of the vehicle form a 26° angle. Vertical and lateral thrusters all use channel thrusters (one at each end, with a symmetrical layout), where the largest positive thrust is 10 kgf, the maximum reverse thrust is 10 kgf, and the maximum input power is 500 W. The thrust of the channel thruster reduces considerably as the AUV longitudinal forward speed increases. In this case, the AUV closes four channel thrusters during rapid sailing to save energy. This study investigates fault diagnosis for the four main thrusters.

T1 and T2 in Fig. 2 are the main horizontal thrusters of the AUV, T3 and T4 are the main vertical thrusters, T5 and T6 are the lateral thrusters, and T7 and T8 are the vertical thrusters.

Table 1
Dimensions and specifications of AUV.

Length	5.6 m
Breadth	1.0 m
Depth	1.8 m
Weight	2.5 t
Operation depth	300 m
Gravity center	$X_g = 0.094$ m $Z_g = -0.023$ m
Buoyancy center	$X_b = 0.093$ m $Z_b = 0.035$ m
Inertia moment	$I_x = 542$ m^4 $I_y = 7580$ m^4 $I_z = 7620$ m^4
Maximum speed	5.5 knot
Propulsion	8 brushless DC thrusters
Sensors	RDI DVL Gyrocompass Depth sensor
OS	VxWorks 5.5
CPU	Intel Pentium 3

2.2. AUV mathematical modeling

The controller design and establishment of the fault diagnosis system require an accurate mathematical model, and the complexity directly affects control quality and fault diagnosis. An overly complex mathematical model results in complicated control and fault diagnosis systems, thereby making construction unfeasible and possibly resulting in overall performance degradation. However, a simple mathematical model cannot reflect the motion characteristics of the system and may degenerate control and fault diagnosis.

The following hydrodynamic equation for an AUV is established:

$$M\dot{\vec{v}} + C\left(\vec{v}\right)\vec{v} + D\left(\vec{v}\right)\vec{v} - g\left(\vec{\eta}\right) = \tau + g_0 \tag{1}$$

where

M – the inertia coefficient matrix of the system, which can meet $M = M_{RB} + M_A \geq 0$;
M_{RB} – the inertia matrix of the carrier, which can meet $M_{RB} = M_{RB}^T > 0$ and $\dot{M}_{RB} = 0$;
M_A – the added mass coefficient matrix, which meets $M_A = M_A^T > 0$;
$C(\vec{v})$ – the Coriolis force coefficient matrix, which meets $C_A(\vec{v}) = -C_A^T(\vec{v})$;
$D(\vec{v})$ – the viscous hydrodynamic coefficient matrix, which meets $D(\vec{v}) > 0 \Leftrightarrow \vec{x}D(\vec{v})\vec{x}^T, \forall \vec{x} \neq 0$;
τ – the control input vector;
g_0 – the static load vector, which is set as 0 to facilitate the study; and.
$g(\vec{\eta})$ – the restoring force/torque vector.

According to the actuator configuration and small rolling size, the AUV mainly uses eight thrusters to lift up and down, slide,

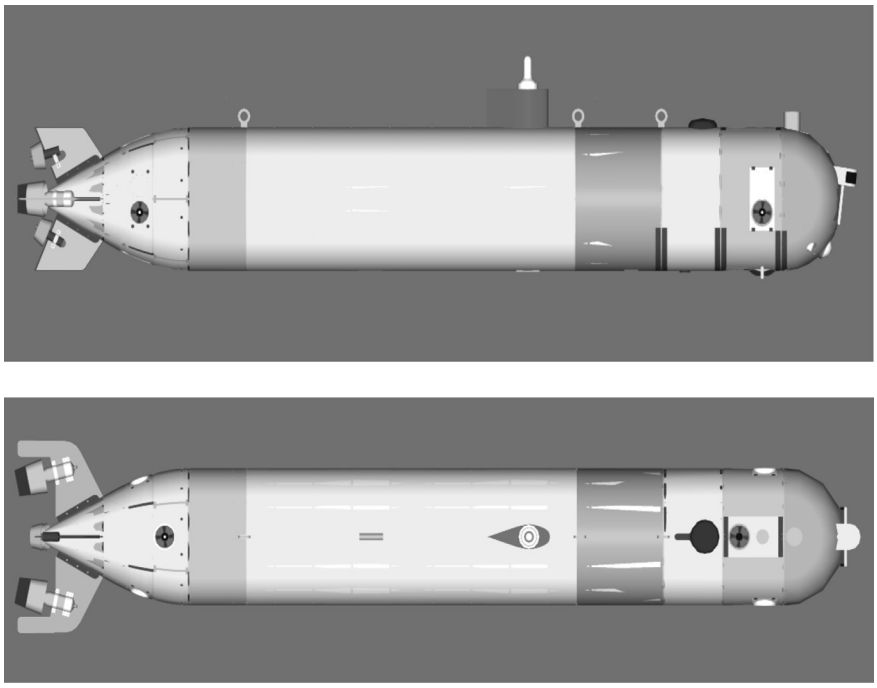

Fig. 1. AUV actuator arrangement.

and make vertical shift, rolling and pitching motions, where the motion model and fault diagnosis can be described approximately through the following six degrees-of-freedom equations. The hydrodynamic coefficients of AUV are difficult to obtain by using the identification method because of the configuration of sensors and the restricted experimental condition. Therefore, we calculated these coefficients by using empirical formulas.

$$\begin{aligned} & m\cdot\left[(\dot{u}-vr+wq)-x_G\cdot\left(q^2+r^2\right)+y_G(pq-\dot{r})+z_G(pr+\dot{q})\right] \\ & \quad=\left[X_{qq}q^2+X_{rr}r^2+X_{rp}rp\right]+\left[X_{\dot{u}}\dot{u}+X_{vr}vr+X_{wq}wq\right] \\ & \qquad+\left[X_{vv}v^2+X_{ww}w^2\right]+X \end{aligned} \tag{2}$$

$$\begin{aligned} & m\cdot\left[(\dot{v}-\omega p+ur)-y_G\left(r^2+p^2\right)+z_G(qr-\dot{p})+x_G(qp+\dot{r})\right] \\ & \quad=\left[Y_{\dot{r}}\dot{r}+Y_{\dot{r}}\dot{p}+Y_{p|p|}p|p|+Y_{qr}qq\right]+\left[Y_{\dot{v}}\dot{v}+Y_{\omega p}\omega p+Y_{ur}ur\right. \\ & \qquad\left.+Y_{r}up\right]+\left[Y_{r}ur+Y_{v|r|}\frac{v}{|v|}\left|\left(v^2+w^2\right)^{1/2}\right||r|\right]+\left[Y_0u^2\right. \\ & \qquad\left.+Y_{v}uv+Y_{v|v|}v\left|\left(v^2+w^2\right)^{1/2}\right|\right]+Y_{vw}vw+Y \end{aligned} \tag{3}$$

$$\begin{aligned} & m\cdot\left[(\dot{w}-uq+vp)-z_G\left(p^2+q^2\right)-x_G(rp-\dot{q})+y_G(rq+\dot{p})\right] \\ & \quad=\left[Z_{\dot{q}}\dot{q}+Z_{rr}r^2\right]+\left[Z_{\dot{w}}\dot{w}+Z_{vr}vr+Z_{vp}vp\right]+\left[Z_{q}uq\right. \\ & \qquad+Z_{w|q|}\frac{w}{|w|}\left|\left(v^2+w^2\right)^{1/2}\right||q|\left.\right]+\left[Z_0u^2+Z_{w}uw\right. \\ & \qquad\left.+Z_{w|w|}w\left|\left(v^2+w^2\right)^{1/2}\right|\right]+\left[Z_{|w|}u|w|+Z_{ww}\left|w\left(v^2+w^2\right)^{1/2}\right|\right. \\ & \qquad\left.\times\right]+Z_{vv}v^2+Z \end{aligned} \tag{4}$$

$$\begin{aligned} & I_x\dot{p}+\left(I_z-I_y\right)qr+m\cdot[y_G\cdot(\dot{\omega}-uq+vp)-z_G\cdot(\dot{v}-\omega p+ur)] \\ & \quad=\left[K_p\dot{p}+K_r\dot{r}+K_{qr}qr+K_{pq}pq+K_{p|p|}p|p|\right]+\left[K_pup+K_rur\right. \\ & \qquad\left.+K_v\dot{v}\right]+\left[K_{vq}vq+K_{\omega p}\omega p+K_{\omega r}\omega r\right]+\left[K_0u^2+K_{uv}uv\right. \\ & \qquad\left.+K_{v|v|}v\left|\left(v^2+\omega^2\right)^{1/2}\right|\right]+K_{v\omega}v\omega+K \end{aligned} \tag{5}$$

$$\begin{aligned} & I_y\dot{q}+(I_x-I_z)rp+m\cdot[z_G\cdot(\dot{u}+wq-vr)-x_G\cdot(\dot{w}-uq+vp)] \\ & \quad=\left[M_{\dot{q}}\dot{q}+M_{rr}r^2+M_{q|q|}q|q|+M_{rp}rp\right]+[M_{\dot{w}}\dot{w}++M_{vr}vr] \\ & \qquad+\left[M_quq+M_{|w|q}\left|\left(v^2+w^2\right)^{1/2}\right|q\right]+\left[M_0u^2+M_wuw\right. \\ & \qquad\left.+M_{w|w|}w\left|\left(v^2+w^2\right)^{1/2}\right|\right]+\left[M_{|w|}u|w|\right. \\ & \qquad\left.+M_{ww}\left|w\left(v^2+w^2\right)^{1/2}\right|\right]M_{vv}v^2+M \end{aligned} \tag{6}$$

$$\begin{aligned} & I_z\dot{r}+\left(I_y-I_x\right)pq+m\cdot[x_G\cdot(\dot{v}-\omega p+ur)-y_G(\dot{u}-vr+\omega q)] \\ & \quad=\left[N_{\dot{r}}\dot{r}+N_{qr}qr+N_{r|r|}r|r|+N_{pq}pq\right]+\left[N_{\dot{v}}\dot{v}++N_{wr}wr\right. \\ & \qquad\left.+N_{vq}vq\right]+\left[N_rur+N_pup+N_{|v|r}\left|\left(v^2+w^2\right)^{1/2}\right|r\right]+\left[N_0u^2\right. \\ & \qquad\left.+N_vuv+N_{v|v|}v\left|\left(v^2+w^2\right)^{1/2}\right|\right]+N_{vw}vw+N \end{aligned} \tag{7}$$

where X, Y, Z, K, M, and N represent the forces generated by the AUV actuator (torque) on various degrees of freedom, including gravity and buoyancy propeller thrust, hydrodynamic fluid movement, and environmental force caused by the underwater vehicle; m refers to the total drainage volume mass

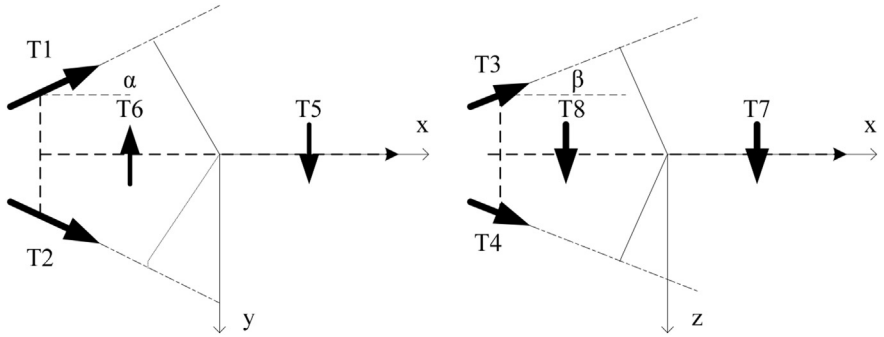

Fig. 2. AUV actuator arrangement. (The horizontal moving surface is on the left, while the vertical moving surface is on the right.).

of the AUV; x_G, y_G, z_G are the AUV gravity coordinates in the hull coordinate system; I_x, I_y, I_z are the moments of inertia of the AUV weight on the hull coordinate system and axis, respectively; and u, v, w, p, q, r are the longitudinal, lateral, vertical, longitudinal angle, and rotary angular velocities of the AUV hull coordinate system, respectively.

$\dot{u}$, $\dot{v}$, $\dot{w}$, $\dot{p}$, $\dot{q}$, and $\dot{r}$ are the accelerated speeds of the corresponding degrees under the AUV hull coordinate system; $X_{\dot{u}}, X_{uu}, Y_{\dot{v}}, Y_v$ are the first- or second-order derivatives of the hydrodynamic hull, which can be obtained through theoretical calculation, constrained model test, identification, and approximate estimation.

We can obtain yaw hydrodynamic coefficients from the identified experiment data by using least squares method. The hydrodynamic coefficients of other DOF are difficult to obtain by using the identification method because of the configuration of sensors and the restricted experimental condition. We calculated these coefficients on the basis of superposition principle and equivalent value principle by using empirical formulas and maps. The hydrodynamic coefficients are shown in Table 2.

Table 2
Non-dimensional hydrodynamic.

Hydrodynamic	Value	Hydrodynamic	Value
$Y'_{\dot{v}}$	−8.154e-2	Y'_v	−2.184e-1
$Y'_{\dot{r}}$	−8.09e-3	Y'_r	1.59e-2
$N'_{\dot{v}}$	−3.876e-3	N'_v	−6.45e-3
$N'_{\dot{r}}$	−1.68e-3	N'_r	4.12e-3
$Y'_{v\|v\|}$	0.2635	$N'_{v\|v\|}$	6.99e-3
$Y'_{r\|r\|}$	0.2331	$N'_{r\|r\|}$	−7.01e-3
$Y'_{v\|r\|}$	−0.2837	$N'_{v\|r\|}$	−8.13e-3
Z'_q	0.01145	$Z'_{\dot{q}}$	−6.40e-3
M'_q	−0.03189	$M'_{\dot{q}}$	2.08e-3
K'_p	2.3e-4	$K'_{\dot{p}}$	1.26e-4

The hydrodynamic Eq. (1) and the AUV state differential equation are combined:

$$\begin{cases} M\dot{\vec{v}} = -C\left(\vec{v}\right)\vec{v} - D\left(\vec{v}\right)\vec{v} + g\left(\vec{\eta}\right) + g_0 + \tau \\ \dot{\vec{\eta}} = J\left(\vec{\eta}\right)\vec{v} \end{cases} \tag{8}$$

Assuming that all the speeds and positions of an AUV can be measured by using a sensor, the measured value can be represented by y. Combining the differential Eq. (7) obtains the state equation of the AUV motion system

$$\begin{cases} \dot{\vec{v}} = M^{-1}\left[-C\left(\vec{v}\right)\vec{v} - D\left(\vec{v}\right)\vec{v} + g\left(\vec{\eta}\right) + g_0 + \tau\right] \\ \dot{\vec{\eta}} = J\left(\vec{\eta}\right)\vec{v} \\ y = h\left(\vec{v}, \vec{\eta}\right) \end{cases} \tag{9}$$

Evidently, the AUV system is a strong nonlinear system that can be represented by the following simplified formula:

$$\begin{cases} \dot{x} = \vec{f}(x) + d + B\tau \\ y = h(x) \end{cases} \tag{10}$$

where $\vec{f}$ is a 12-line matrix function, $\vec{f}(x) = [M^{-1}*[-C(\vec{v})\vec{v} - D(\vec{v})\vec{v} + g(\vec{\eta})]; J(\vec{\eta})]$where the roll angle is set as 0 because this angle is uncontrollable.

x − the vector that comprises 12 controllable motion state variables $x = (u, v, w, p, q, r, x, y, z, \varphi, \theta, \psi)^T$;
τ− the control input τ=$[X, Y, Z, K, M, N]^T$;
B− the input matrix $B = [M^{-1};0]$;
d − the interference term, which includes the static load; and.
y − the value measured by the sensor.

Eq. (9) shows the mathematical model to study the motion and fault diagnosis of AUVs.

3. Basic principle of the Gaussian particle filter and the improved algorithm

The basic idea of the Gaussian particle filter is to assume that the posterior probability density function of the estimated quantity of state is similar to multi-Gaussian distribution; particle filter technology is adopted to obtain relevant parameters and the Gaussian distribution filtering result. The Gaussian particle filter has certain advantages for the strongly nonlinear system of AUVs. However, particle degradation has been restricting the application of the particle filtering algorithm, which is usually solved through the design importance density function and resample. The standard particle filter algorithm adopts the resampling technique, but excessive

particle resample leads to particle exhaustion easily. Gaussian particle filtering is a non-resampling particle filtering algorithm that can avoid these problems.

3.1. Basic principle of gaussian particle filtering

The density of the Gaussian random variable x can be expressed as

$$N\left(x;\mu,\sum\right)=(2\pi)^{-m/2}\left|\sum\right|^{-1/2}\times\exp\left(-(x-\mu)^{T}\sum^{-1}(x-\mu)/2\right)$$

Where x is the dimensional vector of m, μ is the average value of x, and $\sum$ is the covariance matrix of x.

Assuming that the posterior probability distribution at $t-1$ is

$$p(x_{t-1}|y_{t-1})=N\left(x_{t-1};\mu_{t-1},\sum_{t-1}\right)$$

where μ_{t-1} and $\sum_{t-1}$ are the mean and covariance of the posterior probability distribution obtained after acquiring the measured value y_{t-1} at moment $t-1$.

The Gaussian particle filtering algorithm can be used to obtain the posterior probability distribution at time t through the following steps (Han et al., 2010):

(1) Forecast update. The particle set of the posterior probability distribution $p(x_{t-1}|y_{t-1})$ at the moment of $t-1$ $\{x_{t-1}^i,w_{t-1}^i\}(i=1,2,\ldots n$, n are particle numbers, the sample set $\{x_{t-1}^i,w_{t-1}^i\}$ at moment t, and the mean $\overline{\mu}_t$ and covariance $\widehat{\Sigma}_t$ of the prior probability distribution can be obtained according to the state transition equation $p(x_k|x_{t-1}^i)$.

(2) Measurement update. Measurement update involves modifying the prior probability distribution according to the measured values. The particle set $\{x_t^i\}(i=1,2,\cdots n)$ is sampled from the importance density function $q(x_t|y_{0:t})$, and the likelihood probability $p(y_t|x_t^i)$ and prior probability $p(x_t^i|x_{t-1}^i)$ are calculated. The weight expression is then given by

$$w_t^i\propto w_{t-1}^i\frac{p\left(y_t|x_t^i\right)N\left(x_t^i;\overline{\mu}_t,\Sigma_t\right)}{q\left(x_t^i|y_{0:t}\right)}\tag{11}$$

Thus, the posterior probability distribution $p(x_t|y_t)$, mean value μ_t of this distribution, and variance $\sum_t$ can be represented with the particle set $\{x_t^i,w_t^i\}(i=1,2,\cdots n)$.

3.2. Gaussian particle filter search

The importance density function is usually taken as the prior probability density function $p(x_t|x_{t-1})$ to simplify the calculation in the general Gaussian particle filter. Therefore, measurement update does not require resampling, but directly uses particles with prior distribution to calculate the likelihood probability $p(y_t|x_t^i)$ as weights of importance. Given that the current measured value is not considered, the sample extracted from the importance density function deviates from the sample extracted from the posterior probability density function, and the deviation is particularly large at the end or at the peak of the priori probability density function in the likelihood function. UKF is generally used in the prediction update to update the particle set to consider the effect of the measured value, that is, the UKF algorithm is adopted to forecast the updated value of the individual particle $\{x_t^i,w_{t-1}^i\}(i=1,2,\cdots n)$, rather than simply using the state transition equation to update (in the case where only few particles exist).

Given that UKF possesses nonlinear characteristics, the prior probability distribution of a new particle set is closer to the posterior probability distribution. Another method is the use of the UKF algorithm to directly obtain the posterior probability density function as an importance density function, and then the particle set $\{x_t^i\}(i=1,2,\cdots n)$ can be sampled from the importance density function for the measurement update. The former method is adopted in this study, and the specific algorithm is given according to the reference (Schmal and Cheng, 2015).

4. AUV actuator fault diagnosis

4.1. Actuator fault model

The AUV motion system is a strongly nonlinear system that can be expressed as $f(t,x,\mathbf{U})$. The motion state can be partly measured by a sensor and can be represented by $h(t,x)$. The investigated AUV motion nonlinear system can be expressed as

$$\begin{cases}\tilde{x}=f(t,x,\mathbf{U})\\ y=h(t,x)\end{cases}\tag{12}$$

where $f(t,x,\mathbf{U})$ contains six degrees-of-freedom dynamic equations and the equation of the AUV motion; $x=(u,v,w,p,q,r,x,y,z,\varphi,\theta,\psi)$ represents the motion state of the AUV; $\mathbf{U}=(X,Y,Z,K,M,N)$ refers to the control role of the AUV; and y is the measured value.

Given the actuator fault, the control (torque) value of the carrier is lost compared with the output value of the controller; assuming that the amount of loss is $\Delta\mathbf{U}$, $\Delta\mathbf{U}+\mathbf{U}$ is used to substitute U in Eq. (11), and the fault diagnosis model of the actuator is obtained. The discretization of the fault diagnosis model is expressed as

$$\begin{cases}x_{k+1}=f(k,x_k,\Delta U_k+U_k)\\ y_{k+1}=h(k+1,x_{k+1})\end{cases}\tag{13}$$

4.2. Reconstruction of filter

In accordance with the fault diagnosis model, the following filter is established.

$$\begin{cases}\tilde{x}_{k+1}=f(k,\tilde{x}_k,\Delta U_k+U_k+v_k)\\ \tilde{y}_{k+1}=h(k+1,\tilde{x}_{k+1})+n_{k+1}\end{cases}\tag{14}$$

where v_k is the processing noise, and n_k is the measurement noise.

Actuator fault diagnosis is the estimated ΔU_k value. Normally, the mean value of ΔU_k is 0 (Herold et al., 2012), and ΔU_k reflects changes in the controller value when fault occurs. ΔU_k is used as a parameter and is combined with the state for joint estimation. The augmented state vector of the system can be expressed as

$$\chi = (u, v, w, p, q, r, x, y, z, \varphi, \theta, \psi, \Delta X, \Delta Y, \Delta Z, \Delta K, \Delta M, \Delta N)$$

The filter equation can be changed into the following form:

$$\begin{cases} \tilde{x}_{k+1} = f(k, \tilde{\chi}_k, U_k) + v_k \\ \tilde{y}_{k+1} = h(k+1, \tilde{\chi}_{k+1}) + n_{k+1} \end{cases} \tag{15}$$

4.3. Thruster fault diagnosis method based on the Gaussian particle filter

(1) Initialization. The initial expanded state value $\chi_0 = (u_0, v_0, r_0, \Delta X_0, \Delta Y_0, \Delta N_0)$ and covariance value P_0 are given, and the particle set $\{\chi_0^i, 1/N\}(i = 1, 2, \cdots n)$ is sampled from the Gaussian distribution $N(\chi; \chi_0, P_0)$ v is the white Gaussian noise of covariance Q, and n is the white Gaussian noise of covariance R.

(2) Time update. The dynamic system of the UKF algorithm is adopted to update the particles, and in the particle set $\{\chi_{k-1}^i\}(i = 1, 2, \cdots n)$ of the posterior probability distribution, the dynamic system of the UKF algorithm is adopted to update the particles. In the particle set $\{\chi_{k-1}^i\}(i = 1, 2, \cdots n)$ of the posterior probability distribution, the set of particles $\{\chi_k^i\}(i = 1, 2, \cdots n)$ is updated, which means prior probability distribution, and the priori mean value of state $\overline{\mu}$ and covariance $\overline{\sum_k}$ is calculated.

(3) Measurement update. Given that the prior probability density function is adopted as the importance density function, an updated set of particles is directly used as the sampling source of the particle set from the importance density function. The weight of importance w_k^i of the particles takes the likelihood probability density.

$$p(y_k | x_k^i) \approx N\left(y_k; \overline{y}_{k|k-1}, P_{y_{k|k-1}}\right)$$

Moreover, the normalized weight $\overline{w_k^i} = w_k^i / \sum w_k^i$, and the posterior mean μ_k and covariance $\sum_k$ affected by the measured value y_k are calculated.

(4) Fault detection and fault degree estimation. The modified Bayes (MB) algorithm is adopted to process the estimated value of ΔU_k and detect the occurrence of fault in an actuator. The sliding time window method is used to process the fault amplitude (Silveira et al., 2009) of $\Delta \widehat{U}_k$ after a fault occurs.

4.4. Fault detection and degree estimation method

The MB algorithm is adopted to detect actuator faults. When the actuator is working properly, the average loss of control force (moment) is $\Delta \overline{U} = 0$, covariance $\overline{U}$ is the selected noise, and $\Delta U - N(\Delta \overline{U}, \overline{P})$. $\Delta \widehat{U}(k)$ refers to the estimated value of $\Delta U(k)$, $\overline{P}$ is the covariance. The calculation expression is

$$\Delta \overline{\widehat{U}}(k) = \frac{1}{L_1} \sum_{j=1}^{L_1} \Delta \widehat{U}(k-j) \tag{16}$$

where L_1 is the length of the time window. The characteristic values can be expressed as

$$d_{\Delta U}(k) = \frac{S_1(k)}{\overline{P}} - \ln\left(\frac{S_2(k)}{\overline{P}}\right) - 1 \tag{17}$$

where,

$$S_1(k) = \frac{1}{L_1 - 1} \sum_{j=1}^{L_1} \left[\Delta \widehat{U}(k-j) - \Delta \overline{U}\right]^2 \tag{18}$$

$$S_2(k) = \frac{1}{L_1 - 1} \sum_{j=1}^{L_1} \left[\Delta \widehat{U}(k-j) - \Delta \overline{U}(k)\right]^2 \tag{19}$$

The occurrence of fault is determined as follows: fault occurs when $d_{\Delta U}(k) > \beta$, but failure does not occur when $d_{\Delta U}(k) < \beta$. Here, β refers to the threshold value, and different β values are set for various systems and inspection variables.

During failure detection and taking the sliding time window length L_2 and threshold ε, the fault amplitude can be calculated through the following if all $\Delta \widehat{U}(k)$ in the time window is

$$\left|\Delta \widehat{U}(k) - \Delta \widehat{U}(k-1)\right| < \varepsilon \tag{20}$$

The amplitude of the fault is.

$$A = \frac{1}{L_2} \sum \Delta \widehat{U}(k) - \Delta \overline{U} \tag{21}$$

where L_2 and ε are obtained according to several simulation experiments. A large ε can obtain an early fault magnitude, whereas a small ε may cause failure in magnitude estimation (Zhu et al., 2009).

5. Simulation and experimental verification

5.1. Simulation model and parameter setting

The ZS-AUV research object in this study is equipped with pairs of vertical and horizontal thrusters and four main thrusters at the end of the stern. The AUV hydrodynamic parameters can be substituted into the actuator fault model (4) to obtain the simulation model, and then each degree-of-freedom control force (moment) is changed to simulate a fault, as shown in Table 3. In the table, F_x and F_y represent the vertical and horizontal thrusts, respectively, and N is the bow moment. Fault is detected by estimating the change, and the thruster layout and usage condition are combined to locate the fault (only the horizontal movement simulation is presented

Table 3
Control values.

t/s	F_x/N	F_y/N	N (N m)
0–75	1000	200	800
75–100	Decrease by 5 N/s	Decrease by 1 N/s	Decrease by 4 N/s
100–150	1000	200	800
150–300	500	50	600

here). The initial value of the expanded state χ_0 is set as 0 vector, and the initial value of covariance P_0 is set as the identity matrix.

Process noise covariance

$$Q = diag\big([16\times10^{-6}, 81\times10^{-8}, 64\times10^{-8}, 10\times10^{-11}, 49\times10^{-6}, 10\times10^{-8}, 10\times10^{-5}, 10\times10^{-5}, 10\times10^{-5}, 10\times10^{-7}, 10\times10^{-7}, 10\times10^{-11}, 25, 16, 25, 10\times10^{-9}, 25, 25]\big)$$

Measurement of noise covariance

$$R = diag\big([10\times10^{-6}, 10\times10^{-7}, 10\times10^{-7}, 10\times10^{-11}, 10\times10^{-9}, 10\times10^{-8}, 10\times10^{-5}, 10\times10^{-5}, 10\times10^{-7}, 10\times10^{-7}, 10\times10^{-7}, 10\times10^{-11}]\big)$$

When the particle number is N = 10, the total elapsed time is 68 s, and the average time is 0.11 s.

5.2. Analysis of simulation results

Fig. 3 shows the simulation results of the fault diagnosis algorithm in the longitudinal degree of freedom. The figure shows that u is the longitudinal velocity, and ΔF_x is the longitudinal thrust loss. Fig. 3(a) shows that the filter can track the longitudinal velocity of the system, a difference exists between the estimated filter and the longitudinal velocity inferred from the model after 150 s, and the longitudinal speed is reduced; this finding indicates that the longitudinal thrust applied on the surface decreases (simulating the condition in still water). Fig. 3(b) shows that the filtering wave increases rapidly after 150 s, thereby indicating that the longitudinal thrust provided by the actuator for the system is less than the required thrust of the controller, which can preliminarily determine the actuator fault related to the vertical thrust. A 75–100 s proportion adjustment process is set to eliminate the effect on the judgment in the adjustment process. Simulation results show that the longitudinal speed has no residual error [see Fig. 3(a)], the estimated filter thrust loss value is approximately zero [see Fig. 3(b)], and the fault diagnosis is not affected in the adjustment and control processes.

Fig. 3(c) shows the estimated thrust (moment) plane based on the modified Bayesian algorithm. The algorithm time window length is $L_1 = 10$, and the threshold is $\beta = 500$. The program determines that actuator fault occurs at 152 s, that is, the fault is detected in 4 cycles after setting the fault time (each cycle is 0.5 s). The amplitude estimation algorithm (time window length $L_2 = 40$) is then adopted, and the estimated vertical thrust losses at 192 s $\Delta F_x = -533.0$ N (threshold $\varepsilon = 4$); the

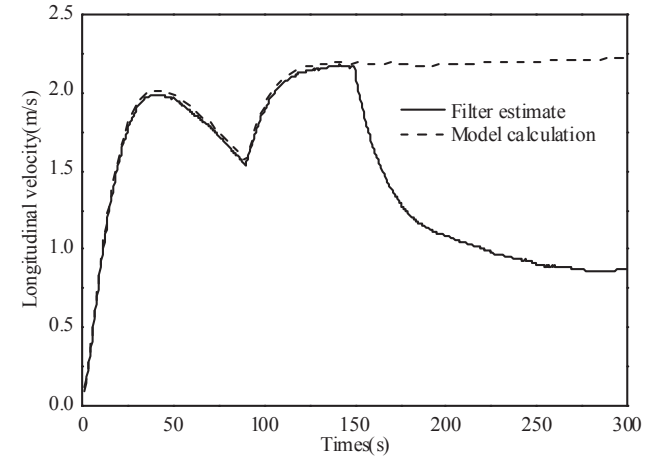

(a) Longitudinal velocity.

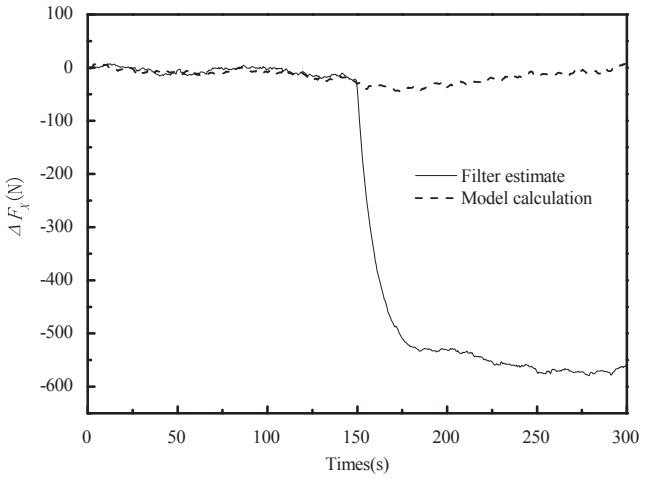

(b) Longitudinal thrust loss value.

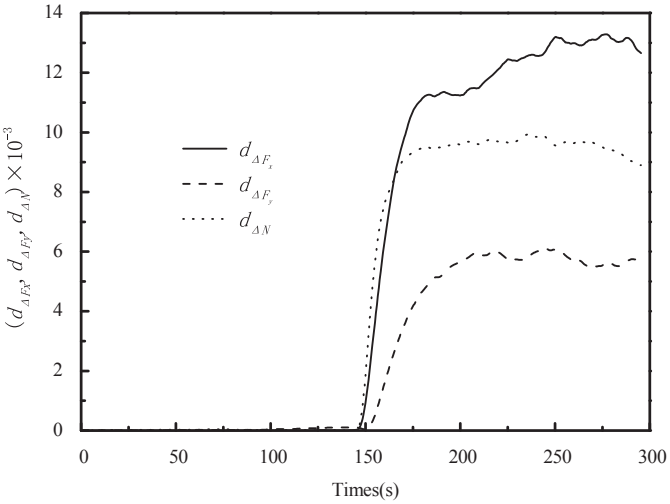

(c) Thrust (torque) loss value.

Fig. 3. Simulation results in the longitudinal direction.

estimated horizontal thrust losses at 182 s $\Delta F_y = -272.9$ N (threshold $\varepsilon = 2$); and the estimated yawing moment loss value at 250 s $\Delta N = -491.5$ Nm (threshold $\varepsilon = 2$). In practical applications, the underwater vehicle layout and the current

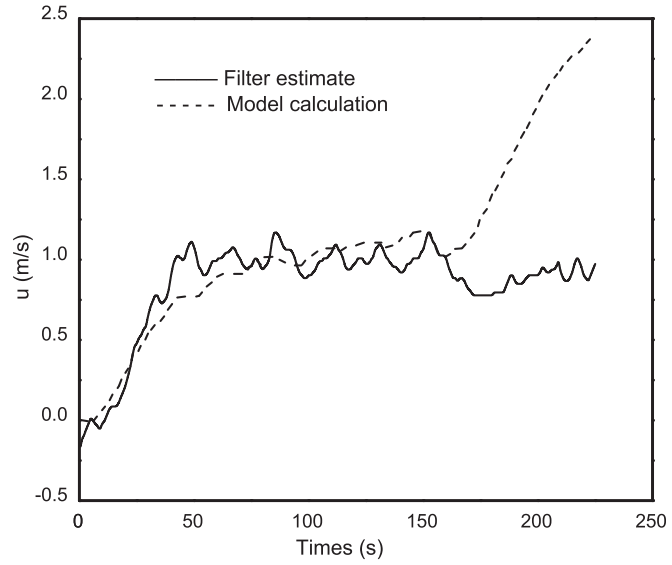

(a) Longitudinal velocity.

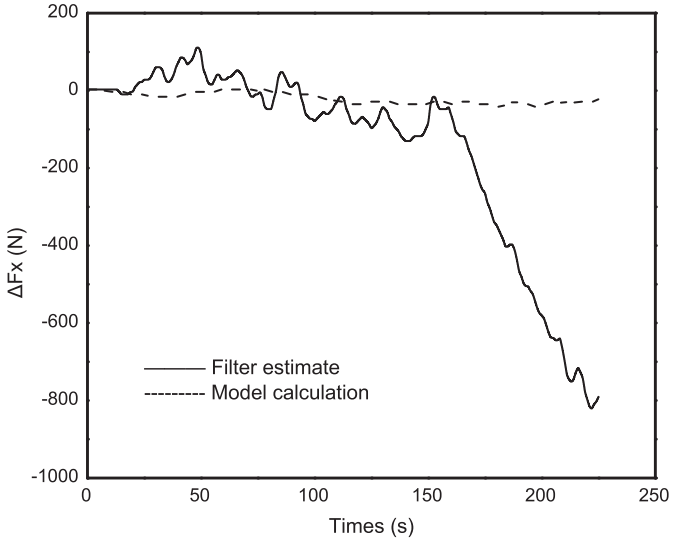

(b) Longitudinal thrust loss value.

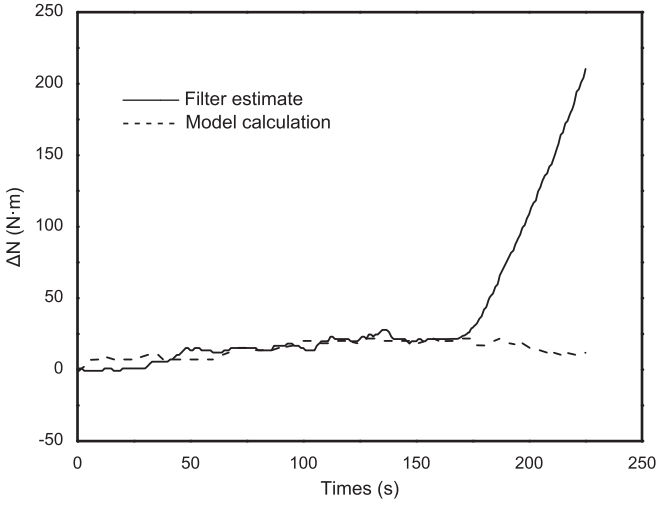

(c) Bow moment loss value.

Fig. 4. Estimation and calculation values of related extended states.

working status should be combined with the usage condition of the actuator or should be further determined.

5.3. Experimental data validation

The real fault data of the AUV with two m/s of speed control are chosen for verification. In Fig. 4(a), the estimated value of the filtering wave has no significant difference from the fault-free estimation before 150 s; the longitudinal speed decreases after 150 s, while the longitudinal velocity calculated by the model increases rapidly; this increase is the combined effect of the actuator fault and controller adjustment. In Fig. 4(b) and (c), the estimated value of the control action increases at 150 s, which leaves the mean value of 0. The improved Bayesian algorithm is adopted to detect the fault, the data window length is $L_1 = 10$, the threshold β is set as 1000 and 500, and the actuator fault is detected at 172 s. Given the length restrictions of sea trial experimental data, the fault magnitude cannot be estimated.

The AUV moves at a constant speed and initially meets the thrust requirement of vertical velocity in speed control. Given the portside main thruster fault, the speed decreases and the thruster moves portside direction, and the controller generates a greater vertical thrust and starboard bow moment. Therefore, the loss in vertical thrust is negative, whereas the loss in the bow torque is positive. According to Fig. 4(b) and (c), fault occurs in the portside main thruster; this occurrence is in accordance with the actual fault set in sea conditions.

6. Conclusion

Simulation tests and actual experimental data indicate that the improved Gaussian particle filter method effectively affects AUV thruster fault diagnosis and that this method can detect fault and estimate fault magnitude quickly. This method affects real-time fault diagnosis positively and can be feasibly applied in fault diagnosis for AUVs. With focus on the working mode and thrust allocation status of AUVs, future research should include an investigation into actuator fault localization and separation.

References

Frank, P.M., 1990. Fault diagnosis in dynamic systems using analytical and knowledge-based redundancy: a survey and some new results. automatica 26 (3), 459–474.

Freitas, N., Dearden, R., Hutter, F., Morales-Menéndez, R., Mutch, J., Poole, D., 2004. Diagnosis by a waiter and a mars explorer. Proc. IEEE 92 (3), 455–468.

Gafurov, S.A., Klochkov, E.V., 2015. Autonomous unmanned underwater vehicles development tendencies. Procedia Eng. 106, 141–148.

Han, S., Zhang, X.L., Chen, L., Wen-Jin, X.U., 2010. Object tracking method based on improved Gaussian particle filter. Syst. Eng. Electron. 32 (6), 1191–1194.

Herold, C., Despiegel, V., Gentric, S., Dubuisson, S., Bloch, I., 2012. Head shape estimation using a particle filter including unknown static parameters. In: VISAPP 2012 – Proceedings of the International Conference on Computer Vision Theory and Applications, 2, pp. 284–293.

Hutt, F., Dearden, R., 2003. The Gaussian particle filter for diagnosis of non-linear system. In: FAC Symposium on Fault Detection, Supervision, and Safety of Technical Processes.

Hutter, F., Dearden, R., 2003. Efficient on-line fault diagnosis for non-linear system. In: International Symposium on Artificial Intelligence, Robotics and Automation in Space.

Schmal, Kendra, Cheng, Haiyan, 2015. Numerical study of a hybrid particle filter. Lect. Notes Eng. Comput. Sci. 2215 (1), 419−422.

Mai, B.L., Choi, H.S., Seo, J.M., Baek, S.H., Kim, J.Y., 2014. Development and control of a new auv platform. Int. J. Control Autom. Syst. 12 (4), 886−894.

Matko, Barisic, Antonio, Vasilijevic, Dula, Nad, 2012. Sigma-point unscented Kalman filtering used for AUV navigation. In: MED 2012-Conference Proceedings, pp. 1365−1372.

Sadeghzadeh Nokhodberiz, Nargess, Poshtan, Javad, 2014. Belief consensus-based distributed particle filters for fault diagnosis of non-linear distributed systems. Proc. Inst. Mech. Eng. Part I J. Syst. Control Eng. 228 (3), 123−137.

Silveira, P.M., Duque, C., Baldwin, T., Ribeiro, P.F., 2009. Sliding window recursive DFT with dyadic downsampling : a new strategy for time-varying power harmonic decomposition. In: Power & Energy Society General Meeting. PES '09. IEEE, pp. 1−6.

Yafe, Han, Mingkai, Yue, Shuhua, Liu, Zhiguo, Sun, 2014. Particle filter resampling algorithms performance analysis under non-Gaussian noise. J. Comput. Inf. Syst. 10 (4), 1751−1758.

Yuan, Fang, Zhu, Da-qi, Ye, Yin-zhong, 2011. Sliding-mode fault-tolerant control method of underwater vehicle based on reduced-order kalman filter. Control Decis. 26 (7), 1031−1035.

Zhu, Hongqian, Hu, Huosheng, Gui, Wei hua, 2009. Adaptive unscented Kalman filter for deep-sea tracked vehicle localization. In: 2009 IEEE International Conference on Information and Automation, ICIA 2009, pp. 1056−1061.